JACS
JOURNAL OF THE AMERICAN CHEMICAL SOCIETY
Communication
pubs.acs.org/JACS

Single-Molecule Fluorescence Microscopy Reveals Local Diffusion Coefficients in the Pore Network of an Individual Catalyst Particle

Frank C. Hendriks,[§,†] Florian Meirer,[§,†] Alexey V. Kubarev,[‡] Zoran Ristanović,[†] Maarten B. J. Roeffaers,[‡] Eelco T. C. Vogt,[†] Pieter C. A. Bruijnincx,[†] and Bert M. Weckhuysen*[,†]

[†]Inorganic Chemistry and Catalysis, Debye Institute of Nanomaterials Science, Utrecht University, Utrecht 3584 CG, The Netherlands

[‡]Centre for Surface Chemistry and Catalysis, Faculty of Bioscience Engineering, KU Leuven, B-3001 Heverlee, Belgium

Supporting Information

ABSTRACT: We used single-molecule fluorescence microscopy to study self-diffusion of a feedstock-like probe molecule with nanometer accuracy in the macropores of a micrometer-sized, real-life fluid catalytic cracking (FCC) particle. Movies of single fluorescent molecules allowed their movement through the pore network to be reconstructed. The observed tracks were classified into three different states by machine learning and all found to be distributed homogeneously over the particle. Most probe molecules (88%) were immobile, with the molecule most likely being physisorbed or trapped; the remainder was either mobile (8%), with the molecule moving inside the macropores, or showed hybrid behavior (4%). Mobile tracks had an average diffusion coefficient of $D = 8 \times 10^{-14} \pm 1 \times 10^{-13}$ m^2 s^{-1}, with the standard deviation thought to be related to the large range of pore sizes found in FCC particles. The developed methodology can be used to evaluate, quantify and map heterogeneities in diffusional properties within complex hierarchically porous materials.

Fluid catalytic cracking (FCC) is one of the major conversion processes in oil refinery, responsible for about half of the gasoline produced worldwide.[1,2] In this process, heavy oil fractions with a high molecular weight are converted into lighter and more desirable products. Spherical catalyst bodies with diameters of 50−100 μm are used, containing zeolite as the active phase within a matrix of silica, alumina and clay. Reactants can enter the catalyst through a complex network of macropores (>50 nm), mesopores (2−50 nm) and micropores (<2 nm).[3]

The accessibility of and mass transport into such a hierarchically porous catalyst greatly influences the overall catalytic activity and final product composition. Therefore, various bulk methods have been developed to determine accessibility and mass transport, such as water titration,[4] physisorption[5] and the so-called accessibility index.[6] The latter method evaluates the adsorption of vacuum gas oil (VGO, i.e., the crude oil fraction with a boiling point range of 340−540 °C)[7] dissolved in toluene into the FCC catalyst. These bulk analysis methods have in common that they provide a macroscopic description of the physicochemical properties, without giving any information about intra- or interparticle heterogeneity.

In the past decades, novel fluorescence microscopy approaches have been developed to study porous materials, including solid catalysts.[8,9] Several of these make use of spatial and temporal separation of diffraction-limited fluorescent emitters improving the resolution to 10 nm.[10] Thus, molecular dynamics can be studied on a nanometer scale, which has led to visualization of diffusional behavior of single molecules in different environments to reveal heterogeneities in diffusion within micro- and mesoporous materials.[11] These techniques have been applied successfully to model materials such as thin films[12] and model catalysts,[13] but the application to real-life catalyst materials has so far been very limited.[14]

Here, we present the first study reporting spatially resolved self-diffusion characteristics of feedstock-like molecules moving in the pore network of a single FCC particle, mapped with nanometer precision. We employed single-molecule fluorescence (SMF) microscopy to monitor the movement of individual molecules within the catalyst particle at 30 nm resolution (Figure 1). This SMF-based approach mimics the bulk experiments used to determine the accessibility index, but, importantly, can also reveal highly localized differences in diffusional behavior.[6] This SMF approach probes self-diffusion rather than diffusion as defined by Fick's law. Both processes are nonetheless governed by the same underlying principle (i.e., random movement of molecules) and ultimately give the same information on macroscopic properties.[15] Thus, "diffusion" will be used below to indicate both diffusion and self-diffusion.

The industrially manufactured FCC catalyst sample under study contains zeolite ZSM-5 as the active phase.[14] An intact single fresh FCC particle of ∼20 μm in diameter was selected to match the microscope's field of view (25 × 25 μm). The pore network of this catalyst was studied using the *N*,*N*′-bis(2,6-dimethylphenyl)-perylene-3,4,9,10-tetracarboxylic diimide (PDI, Figure 1c) probe molecule. The poly aromatic nature and dimensions (Ø 1−2 nm) of this probe are similar to components of VGO,[16] although PDI contains more (polar) functional groups. It has a high photostability and a fluorescence quantum yield close to unity.[17] FCC particles were submerged in a PDI solution of extremely low

Received: July 23, 2017
Published: September 13, 2017

DOI: 10.1021/jacs.7b07139
J. Am. Chem. Soc. 2017, 139, 13632−13635

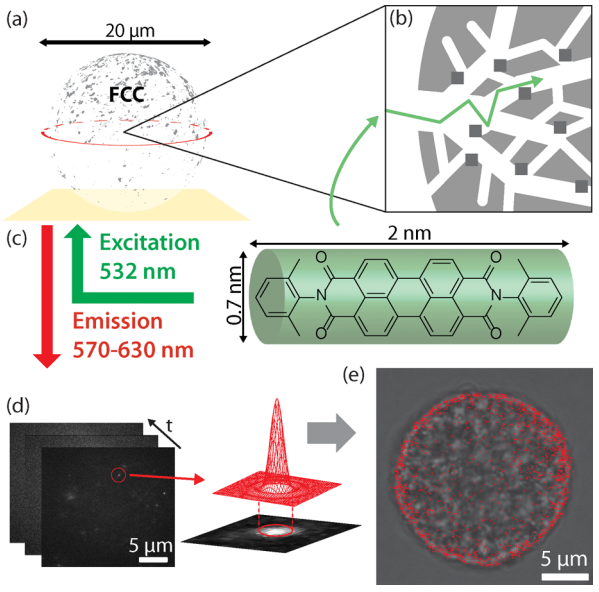

Figure 1. SMF microscopy allowed the location of the feedstock-like probe molecule PDI to be determined within the pore network of a single FCC particle. (a) The whole FCC particle was submersed in toluene in a custom-made cell. (b) Schematic of the pore network of an FCC particle; light gray represents the matrix while dark gray squares represent the embedded zeolites. (c) The PDI probe molecule's dimensions. (d) Fitting the point spread function of each single-molecule event in the recorded fluorescence movies yielded their location and movement. (e) Map of all detected fluorescence events after trajectory analysis overlaid on the bright field transmission image.

concentration (7×10^{-11} M in toluene). This allowed following the movement of individual PDI molecules with an inverted wide field microscope, focused at the middle of the FCC particle to image a complete cross section. Wide field fluorescence microscopy images, showing single molecules as bright fluorescent events (Figure S2) were recorded as movies with a frame rate of 49 frames/s (Figure S3) over a period of 2 h.

A frame-by-frame analysis of these single-molecule fluorescent events yielded the trajectories of the single PDI molecules.[18] The observed movement is a 2-D projection of 3-D movement resulting in a slight underestimation of the step length (see section S4). The maximum displacement of a molecule between two frames (20 ms) was limited to 300 nm, and only tracks consisting of 4 steps or more were considered (Figure S5). While the system was allowed to equilibrate before the measurement, a slow increase in the number of tracks was still observed at the edge of the particle over time, an effect that is most likely caused by the dense crust that surrounds these particles (see below). This is supported by an analysis of the direction of the tracks, which, importantly, showed no evidence for directed molecular movement, indicating no or only a weak concentration gradient (Figure S6). Tracks were subsequently classified using a machine-learning approach (Figure S7).

Figure 2 shows the distribution of the PDI tracks over the central cross section of the FCC particle; a total of 1991 tracks were found throughout the cross section, showing that PDI probe molecules have access to the particle's complete pore network. The edge of the particle nonetheless shows a much higher density of tracks than the center. Both the difference in optical path length in the light-attenuating FCC medium (see section S8) and the dense crust surrounding these particles are thought to contribute to this higher observed density.[19]

Two distinct modes of movement were observed, leading to 3 different types of tracks (Figures 2a and S9). The majority of probe molecules actually showed little movement (Figure 2b). The similarity of these tracks to PDI entrapped in a dense polystyrene film (Figure 2e) and assumed to be nonmoving, suggests that the majority of the PDI molecules in the FCC particle is immobile. Any apparent movement of these immobile molecules is due to the uncertainty in localization of each point in the track. The latter is relatively large at ~30 nm, as imaging the center plane of a whole particle rather than a thin film gives a lower signal-to-noise (S/N) ratio. The fluorescence emission spectrum of the probe molecules inside the particle showed a red shift of 18 nm compared to the emission of molecules in toluene solution, but no change in the relative intensity of the bands (Figure S11). Chemisorption (i.e., by protonation) can therefore be excluded as the main reason for immobility.[20] Physisorption of the probe molecules to the pore wall is then most likely the main reason for a single molecule's immobility, which also explains the presence of hybrid tracks (Figure 2c). Some PDI molecules are completely immobile, suggesting that they could also be trapped in a small pore or cavity. The tracks belonging to immobile PDI were separated from the other tracks by setting a threshold of twice the localization uncertainty (60 nm) to their size (Figure S10). It was found that 1743 tracks (88%) belonged to the immobile category.

The remaining tracks do show considerable movement and mobile molecules (Figure 2d) and ones that switch between immobile and mobile states within one track (hybrid, Figure 2c) can be discerned. Figure 2a shows each of these track types to be fairly homogeneously distributed. Furthermore, there is

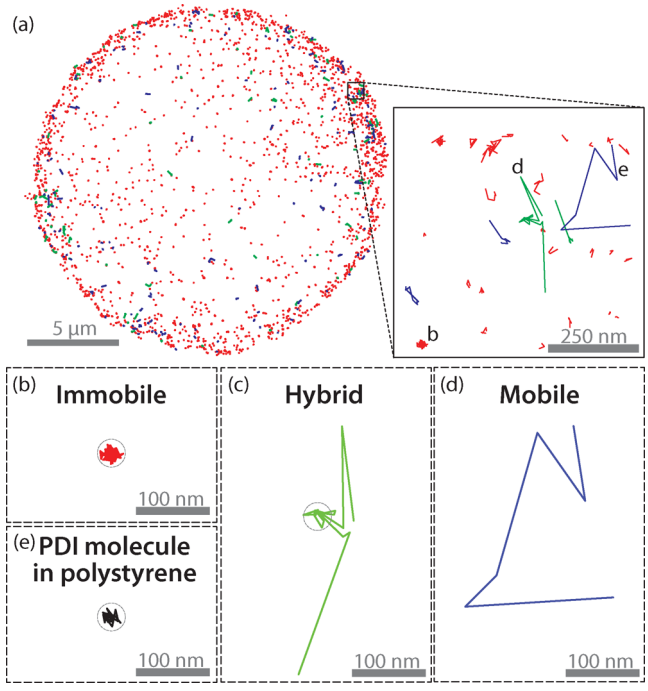

Figure 2. (a) Color-coded map of each recorded PDI track within the FCC particle, showing (b) immobile (red), (c) hybrid (green) and d) mobile tracks (blue). (e) PDI track immobilized in a polystyrene thin film.

DOI: 10.1021/jacs.7b07139
J. Am. Chem. Soc. 2017, 139, 13632−13635

no clear preference in the distance these molecules travel between frames (Figure S10). Pore size analysis by Hg porosimetry (Figure S12) showed that most pores are in the 50−300 nm range, i.e., macroporous. With the micropores of the zeolites being inaccessible for PDI, the observed movement thus originates mainly from molecules present in these macropores. Movement in the smaller (meso)pores falls within the localization uncertainty of the technique and can therefore not be distinguished from immobility. Track separation (Figure S7) classified 160 tracks (8%) as mobile, whereas 88 (4%) belonged to the hybrid type. With 10 steps or 200 ms per average track, the tracks are considerably shorter than in other single particle tracking studies, sometimes reporting seconds-long tracks.[12] Though the immobile tracks show this duration, the mobile tracks are on average much shorter, suggesting that termination of these tracks is caused by out-of-focus movement of the tracked PDI molecule. The estimated focal plane depth is ~500 nm, but may be smaller as the lower S/N causes the localization algorithm to reject some slightly out-of-focus events. Photobleaching is not likely to contribute much to the short average track time as very long (>1 s) tracks are detected for some immobile molecules.[20]

The 2-D movement of each track was analyzed by calculation of the mean square displacement (MSD); the three track types show clearly different MSDs (Figure S13). Notably, the mobile and hybrid tracks show a broad distribution in MSD offset values. With displacement being directly related to a molecule's confinement, this broad MSD distribution can therefore be considered a consequence of the large range of pore sizes present within the FCC catalyst particle (Figure S12).[21] Local and averaged diffusion coefficients D can be obtained by linear fitting of the MSD curves.[22] This bottom-up approach to determine D for a single molecular trajectory provides valuable information about diffusion properties. D gives a measure of mass transfer within the catalyst and is therefore an indicator of catalyst performance.[15,23] With D now available for each track, localized information on the diffusion coefficient can be obtained, as plotted in Figure 3a. Local heterogeneity in D is observed, but no evidence was found that the diffusion coefficient of a molecule depends on its location, for example on the distance of the track from the particle's surface (Figure S14). Large differences in D are also found between tracks of the same type, as evidenced in Figure 3b. Necessarily, D values of all immobile tracks are within localization uncertainty. Interestingly, most hybrid tracks also fall within this category, meaning that for those tracks their immobile part dominates their (time-averaged) diffusion coefficient.

The large number of immobile tracks (88%) suggests relatively strong interactions with the pore walls, which might be the result of the PDI's polar functional groups. Even though experimental data on the bulk diffusion properties of PDI in FCC are not available, our results would thus predict low diffusion coefficients to be observed if determined by bulk measurements as those mentioned above. However, considering that PDI is used here to model the diffusion of VGO molecules in a FCC particle, it should be noted that the VGO components are less polar and thus expected to interact less strongly with the pore walls. With size being most important to diffusion, the nonphysisorbed (i.e., mobile) fraction of the PDI molecules are thus expected to show diffusion behavior similar to VGO molecules, as they have similar dimensions. Indeed, the bulk diffusion coefficient (5×10^{-13} m^2 s^{-1}),[16] measured by adsorption of VGO molecules into FCC is very similar to the

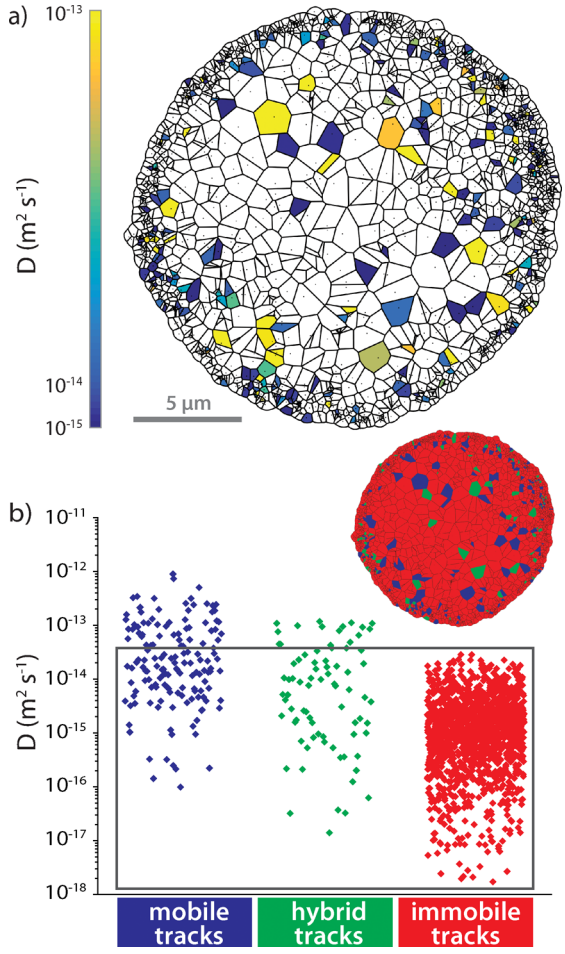

Figure 3. (a) Voronoi diagram showing localized diffusion coefficients in the middle cross section of the FCC particle. Each track's center of mass, indicated with a dot, is surrounded by an area that is closer to that track than to any other. The color of each area indicates the diffusion coefficient, with areas around immobile tracks being white. (b) Diffusion coefficients of each type of track. The gray rectangle includes diffusion coefficients falling within the localization uncertainty of the single-molecule analysis. The inset Voronoi diagram shows the spatial distribution of each track type.

average diffusion coefficient of the fraction of mobile molecules ($8 \times 10^{-14} \pm 1 \times 10^{-13}$ m^2 s^{-1}).

The efficiency of a catalyst particle can be estimated by the Thiele modulus Φ_2 based on the relative influence of the intraparticle diffusion and the reaction rate, and the related effectiveness factor η.[24] The experimentally determined, single molecule-based diffusion coefficient of the mobile fraction of molecules and information available on the FCC process gave a Thiele modulus Φ_2 of 5.4 (see Supporting Information).[25] This is in line with what was previously found for this process, validating our bottom-up approach.[26,27] The calculated effectivity (19%) shows the effect of diffusion limitations on the utilization of the catalyst particle under reaction conditions for molecules with a diameter similar to PDI. Here it is important to note that precracking of large molecules, which occurs in the macro- and mesopores of the particle, will increase the diffusion coefficient of the resulting (smaller) products and improve catalyst efficiency.

In summary, we have visualized single-molecule diffusion inside the pore network of a real-life FCC particle by recording the movement of individual, feedstock-like molecules using

DOI: 10.1021/jacs.7b07139
J. Am. Chem. Soc. 2017, 139, 13632−13635

SMF microscopy. Tracks of these single molecules were found throughout the whole cross section of the FCC catalyst particle. Most PDI probes were found in an immobile, most likely trapped or adsorbed state, with a smaller subset of mobile molecules moving through the pore network of the FCC particle. A large variation in the diffusion coefficient was observed, consistent with the broad range of pore sizes in FCC catalyst particles. We are now in the unique position to map diffusion properties of different types of molecules in real-life, single catalyst particles using SMF microscopy, providing high-resolution physicochemical information on its macropore network. The combination of this approach with complementary, detailed information on the catalyst's inorganic structure can bring structure−mass-transfer−reactivity relationships within individual single catalyst particles or other hierarchically structured materials within reach.

■ ASSOCIATED CONTENT

Supporting Information

The Supporting Information is available free of charge on the ACS Publications website at DOI: 10.1021/jacs.7b07139.

Details of the experiment and data analysis (PDF)
Single molecule movie (AVI)

■ AUTHOR INFORMATION

Corresponding Author

*b.m.weckhuysen@uu.nl

ORCID

Eelco T. C. Vogt: 0000-0003-4556-4283
Pieter C. A. Bruijnincx: 0000-0001-8134-0530
Bert M. Weckhuysen: 0000-0001-5245-1426

Author Contributions

§These authors contributed equally to this work.

Notes

The authors declare no competing financial interest.

■ ACKNOWLEDGMENTS

We thank Albemarle for providing the FCC catalyst particles, Dr. P. Dedecker (KU Leuven) for help with the Localizer software and J. van der Reijen (Utrecht University, UU) and Dr. S. Kalirai (UU) for fruitful discussions. This work is supported by a Netherlands Organization for Scientific Research (NWO) CW-TOP research grant, a NWO Gravitation program and a European Research Council (ERC) Advanced Grant to BMW (No. 321140), The Netherlands Center for Multiscale Catalytic Energy Conversion (MCEC), an ERC Starting Grant (no. 307523) and a Research Foundation-Flanders (FWO) project (G0B9615N) to M.B.J.R. and a NWO VIDI Grant to F.M.

■ REFERENCES

(1) Vermeiren, W.; Gilson, J.-P. *Top. Catal.* **2009**, *52*, 1131.
(2) Vogt, E. T. C.; Weckhuysen, B. M. *Chem. Soc. Rev.* **2015**, *44*, 7342.
(3) Everett, D. H. *Pure Appl. Chem.* **1972**, *31*, 577.
(4) Liu, C.; Tan, Z.; Ding, W.; Zheng, S.; Pang, X.; Sun, S.; Wang, D.; Teng, Q.; Lu, T. Method to Raise the Solid Content of Catalytic Cracking Catalyst Slurry. U.S. Patent 7,727,924B2, June 1, 2010.
(5) Mitchell, S.; Michels, N.-L.; Kunze, K.; Pérez-Ramírez, J. *Nat. Chem.* **2012**, *4*, 825.
(6) Babitz, S. M. Catalyst, a process for its preparation, and its use. U.S. Patent 9534177B2, January 3, 2017.
(7) Altgelt, K. H.; Boduszynski, M. M. *Composition and Analysis of Heavy Petroleum Fractions*; CRC Press: New York, 1993.
(8) von Diezmann, A.; Shechtman, Y.; Moerner, W. E. *Chem. Rev.* **2017**, *117*, 7244.
(9) Janssen, K. P. F.; De Cremer, G.; Neely, R. K.; Kubarev, A. V.; Van Loon, J.; Martens, J. A.; De Vos, D. E.; Roeffaers, M. B. J.; Hofkens, J. *Chem. Soc. Rev.* **2014**, *43*, 990.
(10) Roeffaers, M. B. J.; De Cremer, G.; Libeert, J.; Ameloot, R.; Dedecker, P.; Bons, A.-J.; Bückins, M.; Martens, J. A.; Sels, B. F.; de Vos, D. E.; Hofkens, J. *Angew. Chem., Int. Ed.* **2009**, *48*, 9285.
(11) Zürner, A.; Kirstein, J.; Döblinger, M.; Bräuchle, C.; Bein, T. *Nature* **2007**, *450*, 705.
(12) Rühle, B.; Davies, M.; Lebold, T.; Bräuchle, C.; Bein, T. *ACS Nano* **2012**, *6*, 1948.
(13) Liu, K.; Kubarev, A. V.; Van Loon, J.; Uji-i, H.; De Vos, D. E.; Hofkens, J.; Roeffaers, M. B. J. *ACS Nano* **2014**, *8*, 12650.
(14) Ristanović, Z.; Kerssens, M. M.; Kubarev, A. V.; Hendriks, F. C.; Dedecker, P.; Hofkens, J.; Roeffaers, M. B. J.; Weckhuysen, B. M. *Angew. Chem., Int. Ed.* **2015**, *54*, 1836.
(15) Feil, F.; Naumov, S.; Michaelis, J.; Valiullin, R.; Enke, D.; Kärger, J.; Bräuchle, C. *Angew. Chem.* **2012**, *124*, 1178.
(16) Liu, Z.; Chen, S. L.; Ge, X.; Dong, P.; Gao, J.; Xu, Z. *Energy Fuels* **2010**, *24*, 2825.
(17) Rademacher, A.; Märkle, S.; Langhals, H. *Chem. Ber.* **1982**, *115*, 2927.
(18) Dedecker, P.; Duwé, S.; Neely, R. K.; Zhang, J. *J. Biomed. Opt.* **2012**, *17*, 126008.
(19) Kalirai, S.; Boesenberg, U.; Falkenberg, G.; Meirer, F.; Weckhuysen, B. M. *ChemCatChem* **2015**, *7*, 3674.
(20) El-Daly, S. A. *Spectrochim. Acta, Part A* **1998**, *55*, 143.
(21) Kirstein, J.; Platschek, B.; Jung, C.; Brown, R.; Bein, T.; Bräuchle, C. *Nat. Mater.* **2007**, *6*, 303.
(22) Michalet, X.; Berglund, A. J. *Phys. Rev. E* **2012**, *85*, 61916.
(23) Wallenstein, D.; Fougret, C.; Brandt, S.; Hartmann, U. *Ind. Eng. Chem. Res.* **2016**, *55*, 5526.
(24) Pérez-Ramírez, J.; Christensen, C. H.; Egeblad, K.; Christensen, C. H.; Groen, J. C. *Chem. Soc. Rev.* **2008**, *37*, 2530.
(25) Froment, G. F.; Bischoff, K. B.; De Wilde, J. *Chemical Reactor Analysis and Design*; John Wiley & Sons: New York, 2011; p 720.
(26) Stockwell, D. M. In *Fluid Catalytic Cracking VII: Materials, Methods and Process Innovations*; Occelli, M. L., Ed.; Elsevier: Amsterdam, 2007; p 137.
(27) Jiménez-García, G.; Aguilar-López, R.; León-Becerril, E.; Maya-Yescas, R. *Fuel* **2007**, *86*, 1278.

DOI: 10.1021/jacs.7b07139
J. Am. Chem. Soc. 2017, 139, 13632−13635